International Journal of Mechatronics, Electrical and Computer Technology (IJMEC)
ISSN: 2305-0543 (Online), ISSN: 2411-6173 (Print)
Vol. 11 (42), Oct. 2021, pp. 5065-5073

Damping of Unbalanced Voltage-Caused Vibrations of Induction Motors

* Erwin Normanyo
Department of Electrical and Electronic Engineering,
Faculty of Engineering,
University of Mines and Technology
Tarkwa, Ghana
enormanyo@umat.edu.gh

Jonathan Prince Nkansah
Department of Electrical and Electronic Engineering,
Faculty of Engineering,
University of Mines and Technology
Tarkwa, Ghana
jonathannkansah13@gmail.com

***Abstract*—Squirrel-cage induction motors adapt to a wide range of industrial applications due to their low cost, robustness and low maintenance. It is however expensive to record some damaged parts, especially when ignored incipient vibrations are the cause. Vibrations impede satisfactory operation; with direct proportion to poor power consumption, low efficiency and downtime. A comprehension of the trending works centers on constructional faults and mechanically tuned solutions to vibrations. One of the sources of induced vibration of induction motors is unbalanced voltages. This modulates the ideal characteristics of the motor speed, electromagnetic torque, voltages and stator current in terms of amplitude and frequency. A proactive damping of unbalanced voltage-induced vibrations are proposed in this paper. Hence, an implementation of a designed active power filter using MATLAB/Simulink software to damp the vibrations was carried out. Simulation results confirm the relational effects of unbalanced voltage on torque ripple. Amplitudes of power supply voltage under unbalanced condition are restored with p.u. values of 0.98 and 1.01. Hence, induction motor vibrations due to unbalanced voltage are minimised to tolerable levels.**

***Keywords*— MATLAB/Simulink, Simulation, Squirrel-cage induction motor, Unbalanced voltage, Vibration**

I. INTRODUCTION

Vibration is basically a repetitive motion of a body relative to a reference in equilibrium, when excited by an internal or external force [1]. A body that freely continues this motion even after removing the external source of disturbance does so at its natural frequency. At resonance, the natural frequency of a system coincidentally exists at the same frequency as the external source of disturbance [2]. Consequently, the expected distortions from the vibration escalates within the shortest period of time. The stability, accuracy, anti-wear and lifespan properties of structures and equipment, express an inverse relationship with the intensity of vibrations. These negative effects are amplified at resonance, completely throwing off structures from their engineered designs [1].

On another hand, vibration is useful in the operation of vibratory machines, fault diagnosis, vibration resistance testing of materials and many others [2]. However, outside the likes of these applications, vibration remains a nuisance. Vibration generally occurs to be frequency, phase and amplitude specific [3]. Likewise, unbalanced voltage and torque ripple irregularities will alter the stable spectra of the Squirrel Cage Induction Motor (SCIM) characteristics [4]. A vibratory system can be described as a mass with elastic (spring) and damper elements. The mass and elastic elements (constituents of a free vibratory system) store kinetic and potential energies, respectively. The energy is depleted by the damper element [2].

A SCIM is employed in most industrial applications because of its simple and rugged construction. They are cheaper and reliable; however very costly should there be occurrence of a complete failure of the machine. Among various causes of the IM failures include vibration. Monitoring and appropriately diagnosing motor vibrations can effectively warn against poor power consumption, low efficiency, downtime loss and consequent production costs. Vibrations in a SCIM may result from many factors: Mechanical unbalance, misalignment, bent shaft, eccentricity, cocked bearing or electrical faults as with the windings and power supply. It is practically impossible to predict the cause of the motor vibrations by sound or magnitude. Therefore, providing a system diagnostic that will not only bypass this limitation but also damp the vibrations of the SCIM is a problem solver.

According to authors of [5], an IM is an electromechanical energy converter, capable of transferring input power from its stator to its rotor electric circuits by induction. Hence, the stator and rotor of a SCIM are mechanically disjointed. About 85% of modern industries equip themselves with SCIMs because of their very useful characteristics: Low cost, low maintenance, reasonable small size and good efficiency [5] [6].

A vibrating SCIM is one that probably exists under faulty electrical, mechanical or environmental conditions [5]. The consequences of vibration on the industrial applications of SCIM are directly proportional to downtime, reduced efficiency of operation (power consumption) and unreliable connection to the power grid [7]. Whilst unbalanced voltage, single phasing, phase reversing, power frequency variations, common mode voltage and overload constitute electrical causes of SCIM faults, imbalance, misalignment, wear and looseness of parts constitute mechanical causes. However, environmental causes have to do with foundation problems, ambient temperature and installation mishaps [5][8][9].

Article History:
Received Date: Jul. 05, 2021, Accepted Date: Aug. 03, 2021, Available Online: Oct. 01, 2021

Vibrations due to unbalanced voltage result from running the SCIM. Either these vibrations can be caused by the SCIM or any secondary equipment like converters for SCIM control [8]. By definition, it implies that they are disjoint from the group of vibrations that develop from the construction of a SCIM. Although mechanical faults contribute to the adverse generation and propagation of vibrations, they mostly depend on the construction or age of the SCIM. Nonetheless, mechanical coupling, wear and misalignment can be cited among the few mechanical faults. Electrical faults during operation affect the performance and lifespan of the SCIM. When the lifespan is affected, mechanical faults aggravate. Consequently, vibration intensifies along with all its detriments. It will therefore benefit to mitigate incipient electrical faults, which will proactively mitigate other probable vibration sources.

II. RELATED WORKS

In terms of mitigation methodologies, authors of [3] in employing the measurement of vibration parameters at reduced voltages in their research, effectively separated electrical from mechanically induced vibrations. Electrically induced vibrations occur at frequencies twice that of the line frequency. Certain vibration develops from faults that create conditions in which a three-phase SCIM will not be allowed to continue operating. Such cases are with the single phasing and phase reversal faults. Hence, these faults will rather be removed other than damping their consequent vibration effects. In [10], authors showed superiority of fuzzy logic controller over proportional-integral (PI) controller in using shunt active filters to mitigate unbalanced voltages and harmonics as sources of common electrical faults. Likewise, Prasad and Tilak [11] looked at voltage unbalance and harmonics as outcomes of dynamic load pressure on power system uncertainty and called for integration of distributed generation (DG) to reduce system overload and improve the voltage profile. The SCIM as a dynamic load in the power system was not considered.

However, mitigation of vibrations of SCIMs are reported in the literature in recent times. A number of recent publications centered on vibration mitigation [9][12-14]. Authors of [9] considered a 5-phase IM in reducing radial, axial and tangential vibrations of the IM by utilising a space vector pulse width modulation technique to eliminate common mode voltages, which are causes of the vibrations via the motor bearings. In [12], the researcher considered dynamic rotor eccentricities in the mathematical modelling of soft mounted IM under forced vibrations without regard to the electromagnetic field, bearing housing or rotor rotating damping. In [13], author conducted theoretical analysis of vibration control of greater than 1 MW rating to achieve significant reduction of bearing and foundation resonances considered as sources of escalation of IM vibrations. Research by Xu *et al.* [14] strongly suggested that parallel circuit and damping windings methods are effective approaches for the suppression of electromagnetic vibrations compared to subdomain analysis, magnetic equivalent circuit, virtual work principle and finite element analysis methods. Other researchers point at torque ripples, which serve as outcomes of unbalanced voltages hence, influence the level of IM vibrations. In this regard, Rosić *et al.* [15] practically implemented torque ripples mitigation of the IM on digital signal processing (DSP) platform. Their approach could not deal with issues of high torque, current ripple and variable frequency. Discrete voltage vector control was then proposed as a solution.

Summarily, vibration of the SCIM clearly impedes its satisfactory industrial operation. Although these vibrations may result from mechanical and electrical faults, most literature dominantly handle the mitigation of vibrations caused by mechanical faults. Contrarily, a narrower scope of research on the response of an operating SCIM to vibration parameters exists. Electrical faults are outstanding compared to the mechanical faults with regard to categorising vibrations. The focus of this paper therefore, is to determine unbalanced voltage-induced vibrations from the analysis of vibration spectrum, model and simulate the vibration condition of SCIM using MATLAB/Simulink software and develop a damping system based on series active power filter (APF) located between the source of power supply and the SCIM for the control of unbalanced voltage-induced vibrations. The rest of this paper is organised as follows: Section 2 expounds on the design concept and criteria, selection of filter, mathematical modelling of the series APF and computer simulations, all as the materials and methods used in this research. Section 3 gives the simulation results and aptly discusses them. Section 4 concludes on the outcome of this research on damping of unbalanced voltage-induced vibrations of SCIMs.

III. METHODOLOGY

A. Design Concept and Criteria

Fig. 1 presents the design concept towards damping of the vibration of SCIM. The filter is purposed to attenuate the unusual frequencies inherent in the power source. The supply is considered as the output of a power converter used in the control of the SCIM [16]. The fast Fourier transform (FFT) is employed to distinguish the desired and the undesired characteristics [17].

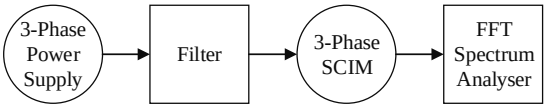

Fig. 1. A block diagram of the design concept

The design criteria is three-fold: Attenuate irregular frequencies within power supply to the SCIM stator, minimise rippling torque and unwanted speed characteristics and thirdly, restore amplitude instabilities that destabilise the SCIM. Additionally, the model is to display the frequency response of the system under normal and unbalanced voltage-induced vibration conditions. Based on the design criteria, an appropriate selection of a filter unit is prerequisite to achieving the set targets. This development climaxed a resolution; such that the tenets of the research are narrowed to relating the efficiency of the filter to the damping of the

IEEE Office - SEET Complex, Federal University of Technology, Owerri, Nigeria, https://aeuso.org
EISSN: 2305-0543, PISSN: 2411-6173

vibrations. A proactive approach to solving any problem minimises the need for system overhaul.

The following baseline assumptions are adopted:

1. The mechanical conditions of the SCIM remain constant.
2. The SCIM operates together with other equipment in a power system.
3. The frequency spectra of the stator current and voltage, torque and speed waveform, serve as vibration indicators of the SCIM.

Propounding unbalanced voltage as the source of vibration requires damping techniques relating to power quality control [4]. Unbalanced voltage results in torque ripple. Hence, the design concept aims to minimise the measure of these irregularities within the power supply to the SCIM.

B. Selection of Filter

Considering the two types of filters: Active and passive filters, the selection criteria of filters are based on the bandwidth of operation, adaptation and elimination of resonance. Passive filters have very useful applications however, they require tuning to specific harmonic frequencies before they can operate. For varying frequencies, they are rendered useless. Then again, there is the tendency of resonance of the passive filter with the source impedance. This generates harmonics within the power system [18]. With these consi-derations, the APF is selected over the passive filter. The series APF is employed to mitigate the incidence of unbalanced voltages that result in SCIM vibrations. This is achieved by injecting compensating current into the power system under fault conditions. Fig. 2 (modified after Ankita *et al*. [19]) represents the series APFs configured into the supply system of SCIM.

C. Mathematical Modelling

a. Modelling of the Series Active Power Filter

The Equations (1) to (5) are employed in the modelling of the series APF.

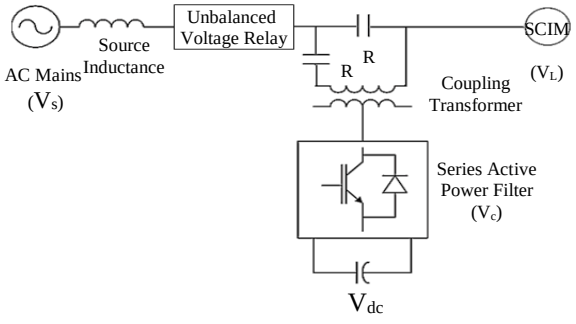

Fig. 2. Configuration of the squirrel-cage induction motor with the series active power filter

$$V_s = V_L \qquad V_c = V_L \tag{1}$$

$$\%V_u = \frac{\text{maximum deviation from the average voltage of the phases}}{\text{average voltage}} \times 100 \tag{2}$$

$$\text{p.u.} = \frac{V_s}{V_n} \tag{3}$$

$$V_{npf} = V_{nrms}\sqrt{\frac{2}{3}} \tag{4}$$

$$V_{c\_ref} = k\,(V_s - V_m) \tag{5}$$

where, V_s, V_L and V_c are AC mains, SCIM and compensating voltages, respectively in volts (V), $\%V_u$ is percentage voltage unbalance, p.u. is per unit value, V_n is nominal voltage in volts (V) V_{npf} and V_{nrms} are peak and nominal rms voltages per phase, respectively (V), V_{c_ref} and V_m are compensating reference and modulated voltages, respectively in volts (V) and k is gain factor.

b. Modelling of the Squirrel Cage Induction Motor

The dynamic model of the stator of the SCIM is represented in its natural coordinates (a, b and c) by Equations (6), (7) and (8) [20].

$$U_{sa} = i_{sa} \times R_{sa} + \frac{dY_{sa}}{dt} \tag{6}$$

$$U_{sb} = i_{sb} \times R_{sb} + \frac{dY_{sb}}{dt} \tag{7}$$

$$U_{sb} = i_{sb} \times R_{sb} + \frac{dY_{sb}}{dt} \tag{8}$$

where, U_{sa}, U_{sb} and U_{sc} are stator voltages of phases a, b and c, respectively in volts (V), i_{sa}, i_{sb} and i_{sc} are stator currents of phases a, b and c, respectively in amps (A), $R_{sa} = R_{sb} = R_{sc}$ are stator resistances of phases a, b and c, respectively in ohms (W), Y_{sa}, Y_{sb} and Y_{sc} are total stator fluxes of the phases a, b and c, respectively in Weber (Wb). A vector representation of the dynamic model of the SCIM stator is presented in Equation (9). Likewise, the model of the rotor along its natural coordinates is presented as a vector using Equation (10) [20].

$$\vec{U}_S = \vec{i}_S \times R_S + \frac{d\vec{Y}_S}{dt} \tag{9}$$

$$\vec{U}_r = \vec{i}_r \times R_r + \frac{d\vec{Y}_r}{dt} \tag{10}$$

where, $\vec{U}_s$ and $\vec{U}_r$ are stator and rotor vector voltages, respectively in volts (V), $\vec{i}_s$ and $\vec{i}_r$ are current vectors of stator and rotor respectively in amps (A), R_s and R_r are stator and rotor resistances, respectively in ohms (W), $\vec{Y}_S$ and $\vec{Y}_r$ are stator and rotor flux vectors, respectively in Weber (Wb). Korondi *et al*. [20] expresses the flux vector of

IEEE Office - SEET Complex, Federal University of Technology, Owerri, Nigeria, https://aeuso.org
EISSN: 2305-0543, PISSN: 2411-6173

the stator and rotor, in Equations (11) and (12), in their natural coordinate system. Hence, the Equations (9), (10), (11) and (12) all together represent the general SCIM equations:

$$\vec{\Psi}_S = \vec{i}_S \times L_S + \vec{i}_r \times e^{jx} \times L_m \quad (11)$$

$$\vec{\Psi}_r = \vec{i}_r \times L_r + \vec{i}_S \times e^{-jx} \times L_m \quad (12)$$

where, L_s is three-phase resultant inductance of the stator in henry (H), L_r is three-phase resultant inductance of the rotor in henry (H), L_m is three-phase mutual inductance in henry (H). Considering $\vec{\Psi}_r$ and $\vec{i}_s$ as state variables, Equation (13) is a state space model developed from the dynamic model of the SCIM in the d-q (direct quadrature) coordinate system [20]. The usefulness of these equations are realised when modelling the SCIM in MATLAB/Simulink software [21].

$$\frac{d}{dt}\begin{bmatrix} i_{sd} \\ i_{sq} \\ \Psi_{rd} \\ \Psi_{rq} \end{bmatrix} = \begin{bmatrix} \frac{\bar{R}}{L_s s} & 0 & \frac{L_m R_r}{L_s s L_r^2} & \frac{L_m w_r}{L_s s L_r} \\ 0 & \frac{\bar{R}}{L_s s} & -\frac{L_m w_r}{L_s s L_r} & \frac{L_m R_r}{L_s s L_r^2} \\ \frac{L_m R_r}{L_r} & 0 & -\frac{R_r}{L_r} & -w_r \\ 0 & \frac{L_m R_r}{L_r} & w_r & -\frac{R_r}{L_r} \end{bmatrix} \begin{bmatrix} i_{sd} \\ i_{sq} \\ \Psi_{rd} \\ \Psi_{rq} \end{bmatrix} + \begin{bmatrix} \frac{1}{Ls} & 0 \\ 0 & \frac{1}{Ls} \\ 0 & 0 \\ 0 & 0 \end{bmatrix} \begin{bmatrix} u_{sd} \\ u_{sq} \end{bmatrix} \quad (13)$$

where, i_{sd} and i_{sq} are stator currents of the d-q axis (A), Ψ_{rd} and Ψ_{rq} are rotor fluxes of the d-q axis (Wb), $\vec{R}$ is rotor resistance vector (Ω), $\bar{s} = 1 - L_m^2/(L_s \times L_r)$ is total leakage coefficient and u_{sd} and u_{sq} are stator voltages of the d-q axis (V).

D. Computer Simulations

Simulations on the damping of voltage unbalance as source of SCIM vibration investigated the time and/or frequency-based responses of the system for conditions under desired baseline characteristics of the AC mains and SCIM and unbalanced voltage source to the SCIM with and without the series APF. The SCIM speed, electromagnetic torque and mechanical load torque are related in Equation (14) and Equation (15) [21]. For the unbalanced voltage condition, the mechanically coupled load was 20 Nm.

$$T_e = T_L + \frac{2}{n} J \frac{dw_r}{dt} \quad (14)$$

$$N_r = w_r \times \frac{30}{p} \quad (15)$$

where, T_e and T_L are electromagnetic and mechanical load torques, respectively in newton-meter (Nm), n is number of poles of SCIM, w_r and N_r are rotor angular speed in rad/s and SCIM speed in rpm, J is rotor inertia in kgm^2.

In order to simulate unbalanced voltage, the Three-Phase Programmable Voltage Source (TPPVS) block in MATLAB/Simulink was used. In modelling the unbalanced voltage condition, the source was programmed to supply under fault between 0.1 s – 0.2 s. Table 1 presents the parameters and their respective values with modelling the SCIM using the Asynchronous Machine SI Units block in MATLAB/Simulink. Table 2 gives values of parameters used in the simulation of unbalanced voltage condition with an integrated series APF. Fig. 3 is the Simulink model of the SCIM under unbalanced voltage condition with the series APF filter integrated for mitigating the consequent vibrations.

TABLE 1. MODEL PARAMETERS OF SQUIRREL CAGE INDUCTION MOTOR

SN	Parameter	Value	SN	Parameter	Value
1.	Power (kW)	7.5	7.	Stator Inductance (H)	0.003045
2.	RMS Voltage (V)	400	8.	Rotor Resistance (Ω)	0.7402
3.	Peak Voltage (V)	326.599	9.	Rotor Inductance (H)	0.003045
4.	Frequency (Hz)	50	10.	Mutual Inductance (H)	0.1241
5.	Rotor Speed (rpm)	1440	11.	Pole Pairs	2
6.	Stator Resistance (Ω)	0.7384	12.	Input Mechanical Load Torque (Nm)	20

(Source: Anon., 2019 [22])

TABLE 2. VALUES OF PARAMETERS USED IN THE SIMULATIONS

SN	Parameter	Value	SN	Parameter	Value
1.	Line Impedance (Ω)	1.00	7.	Coupling Inductance (mH)	1.5
2.	Transformer Rated Power (MVA)	10	8.	DC Voltage (V)	80
3.	Transformer Rated Voltage (V)	400	9.	Mechanical Load Torque (Nm)	20
4.	Gain Factor	0.5	10.	Branched Resistance (Ω)	5
5.	Relay Switch-On Point	0.01	11.	Branched Capacitance (μF)	20
6.	Relay Switch-Off Point	-0.01			

(Source: Anon., 2019 [22]; Budhrani *et al*., 2018 [23])

IEEE Office - SEET Complex, Federal University of Technology, Owerri, Nigeria, https://aeuso.org
EISSN: 2305-0543, PISSN: 2411-6173

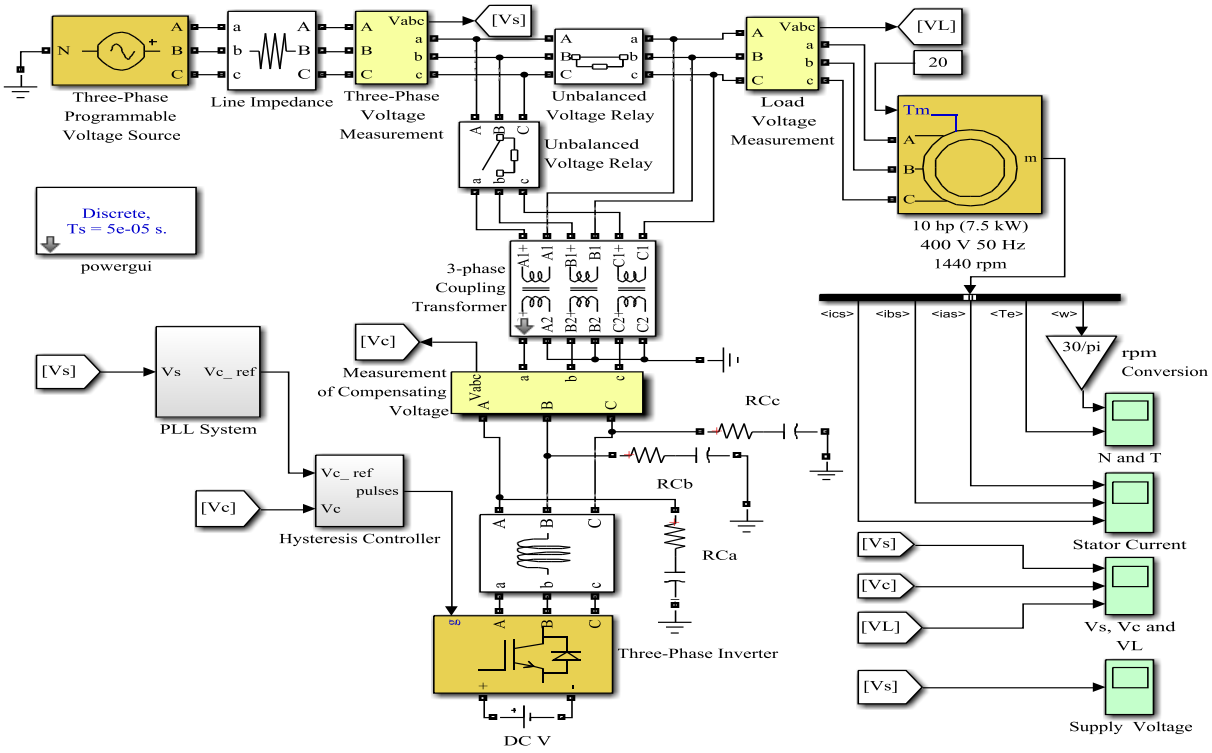

Fig. 3. Simulink model of the squirrel-cage induction motor under unbalanced voltage condition with the series active power filter

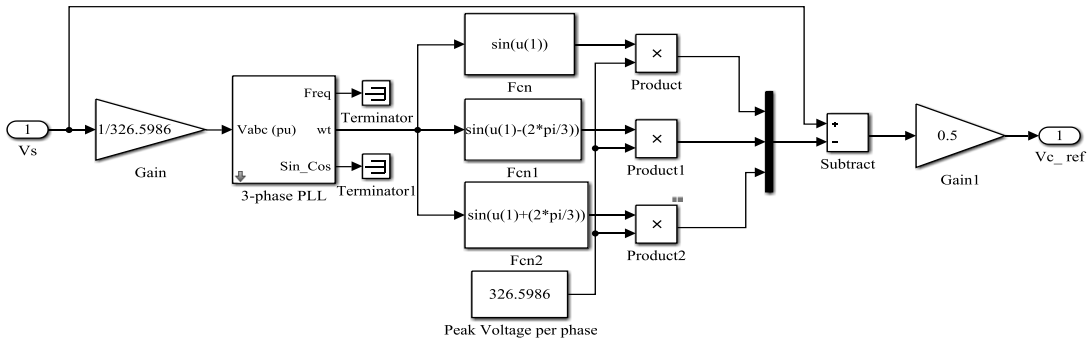

Fig. 4. Simulink model of the phase-locked loop system

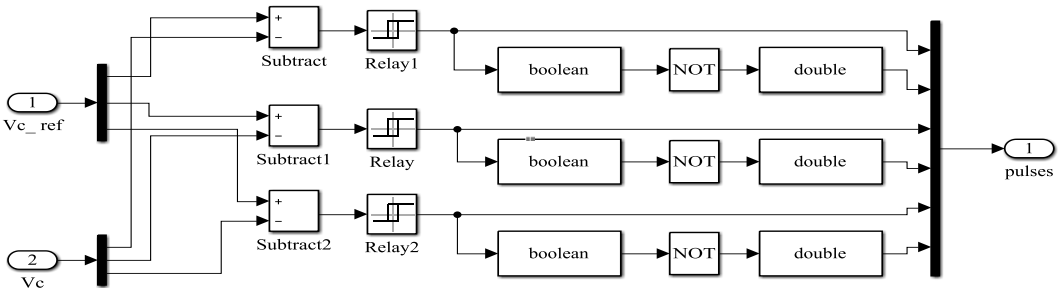

Fig. 5. Simulink model of the hysteresis controller

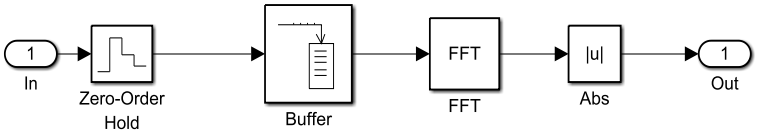

Fig. 6. Simulink model of fast Fourier transformation

IEEE Office - SEET Complex, Federal University of Technology, Owerri, Nigeria, https://aeuso.org
EISSN: 2305-0543, PISSN: 2411-6173

Major blocks within the series apf system include the phase-locked loop system of the reference voltage generation module (Fig. 4) and hysteresis controller module (Fig. 5). The fast Fourier transformation module is represented in simulink software as shown in Fig. 6.

IV. SIMULATION RESULTS AND DISCUSSION

A. Simulation Results

a. Baseline Characteristics under Normal Squirrel-Cage Induction Motor Operation

Fig. 7 presents the waveforms of the SCIM speed and electromagnetic torque under 400 V supply, 20 Nm coupled mechanical load, at a speed of 1440 rpm and without sources of vibration. Fig. 8 gives the frequency spectrums of the SCIM torque and stator current without sources of vibration.

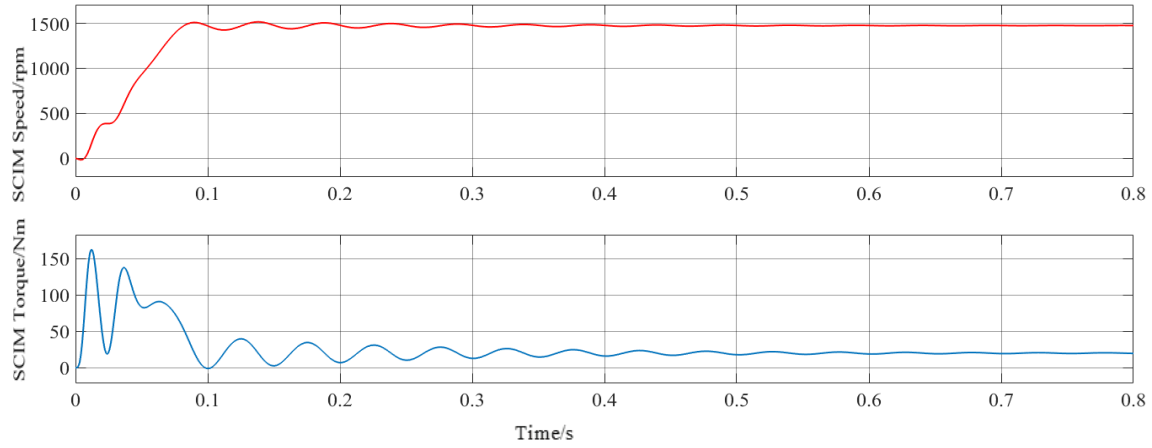

Fig. 7. Waveforms of speed and torque under normal squirrel-cage induction motor operation

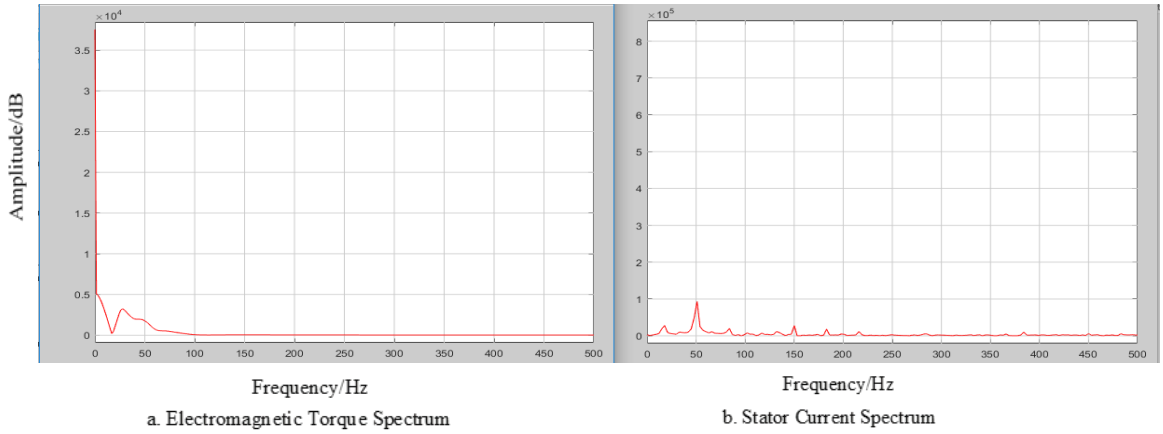

Fig. 8. Torque and stator current frequency spectrums without sources of induced vibrations

b. Unbalanced voltage condition without series active power filter

The type of voltage unbalance considered was an all three-phase instability, occurring at specific intervals and at varying magnitudes. The unbalance condition occurs between t = 0.1 s and t = 0.2 s. Fig. 9 is the waveform of the supply voltage under unbalanced condition, due to voltage instability in all three phases. Fig. 10 is the response of the speed and electromagnetic torque of the SCIM under voltage unbalance conditions, without any damping measure.

c. Unbalanced voltage condition with series active power filter

Fig. 11 is the waveform of the supply voltage, compensating voltage and load voltage under unbalanced condition after integrating with the series APF. Fig. 12 is the response of the speed and electromagnetic torque of the SCIM under voltage unbalance conditions with the series APF.

IEEE Office - SEET Complex, Federal University of Technology, Owerri, Nigeria, https://aeuso.org
EISSN: 2305-0543, PISSN: 2411-6173

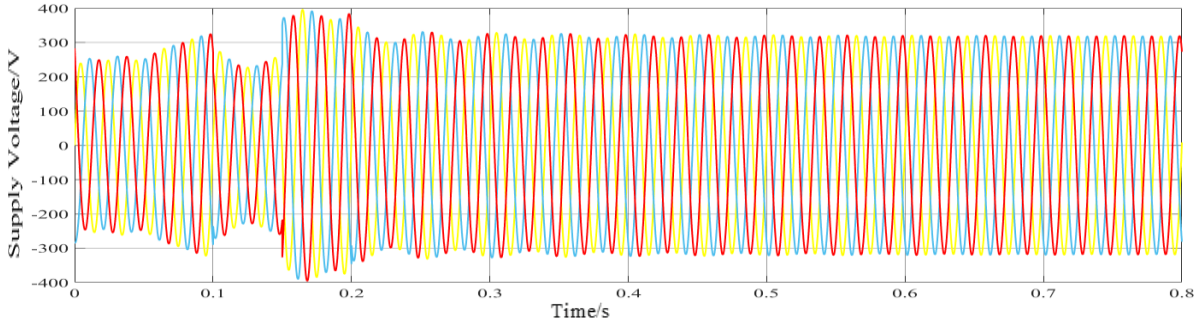

Fig. 9. Three-phase instability of the supply voltage

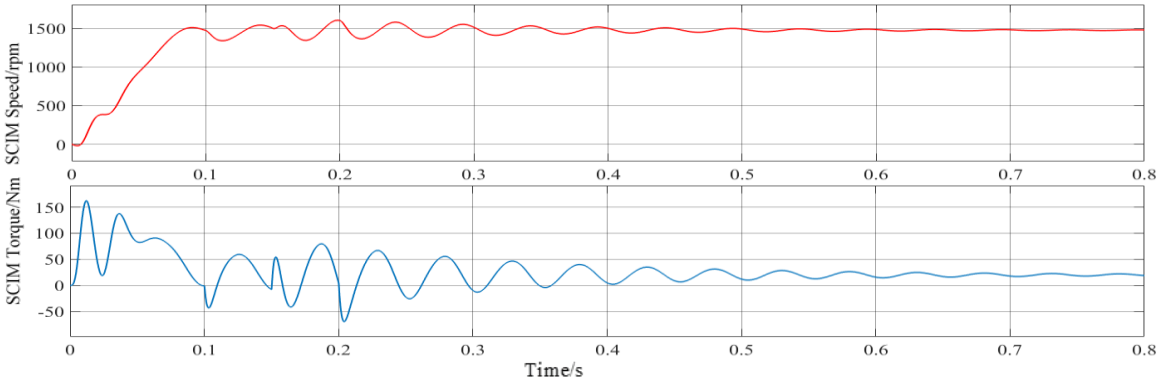

Fig. 10. Responses of squirrel-cage induction motor speed and torque to unbalanced voltage supply

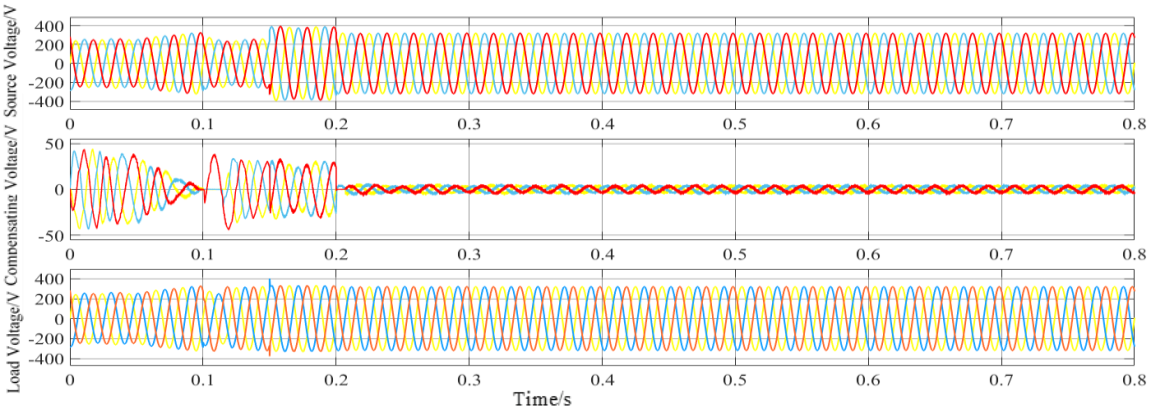

Fig. 11. Source, compensating and load voltages under unbalanced voltage condition with series active power filter

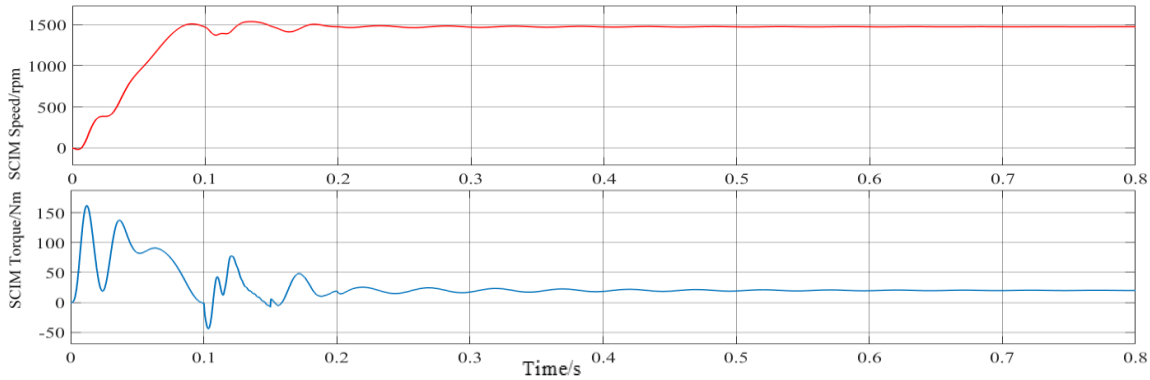

Fig. 12. Squirrel-Cage Induction Motor Speed and Torque under Unbalanced Voltage Condition with Series Active Power Filter

IEEE Office - SEET Complex, Federal University of Technology, Owerri, Nigeria, https://aeuso.org
EISSN: 2305-0543, PISSN: 2411-6173

B. Discussion of Simulation Results

The simulation results of Fig. 7 showed the baseline characteristics in terms of SCIM speed and electromagnetic torque. On start, between t = 0 – 0.1 s, the speed rose to 1509 rpm at peak time, t = 0.09 s. The torque underwent turbulent transient characteristic after maximum 162 Nm at peak time, t = 0.012 s. Between t = 0.1 s – 0.2 s, the speed overshot again to 1516 rpm however, oscillating within 1471 ± 45.6 rpm. The torque decreased from a maximum of 39.6 Nm at t = 0.125 s to 7 Nm at t = 0.2 s. Hence, the torque oscillated with values about 23.3 ± 16.31 Nm. From t = 0.2 s – 0.8 s, the speed and torque gradually settled to the rated values of 1440 rpm and 20 Nm, respectively.

The introduction of frequency analysis enabled the identification of superimposed signal constituents at their occurring frequencies with respective amplitudes of intensity. Fig. 8a is a typical characteristic of SCIM having no sources of vibration from the power supply. The peak at 0 is the mean power component. The other peaks between the 0 and 50 Hz are as a result of the asymmetrical nature of the power supply or SCIM. The peak value occurring at 50 Hz in Fig. 8b, is an indication of the dominant fundamental frequency component of the ideal power supply. Likewise, the subtle projections observed within the frequency frame are due to the construction of the SCIM or auxiliary equipment. This includes the existing filter present, even at normal operating conditions.

The programmed voltage unbalance modulated the amplitude distortion in the supply voltage shown in Fig. 9, between t = 0.1 s – 0.2 s. As a result of the series connection of APF between the power supply and the SCIM at this instance, the load voltage also assumed this same characteristic. At t > 0.2 s, the voltage amplitude of the three phases continued to fluctuate within 330.65 ± 15.14 V until at average time t = 0.655 s, where 97.86% of the ideal peak voltage was collectively measured.

Changes were observed from Fig. 7 with reference to Fig. 10 under vibration due to unbalanced voltage. However, before the initiation of the fault at t = 0.1 s, the transient characteristics of speed and electromagnetic torque remained unchanged. Between t = 0. 1 s – 0.2 s, changes were observed both in terms of speed and torque. The speed was observed to oscillate within 1471 ± 131.95 rpm. Likewise, torque oscillation occurred outside the ideal 23.3 ± 16.31 Nm range and with six pairs of zero-crossings. Clearly, these are evident consequences of undesired vibration. Then again, persistent oscillations were observed with speed and torque, even after the programmed time of the unbalanced voltage had elapsed for t > 0.2 s.

The integration of the series APF effected a load voltage response to a compensating voltage in Fig. 11. The source and load voltages exhibited magnitudes for t < 0.11 s. However, the compensating effect of the series APF only started to take effect from t = 0.12 s – 0.2 s. At t = 0.12 s and from a common phase, the calculated p.u. values for the source and load peak voltages were 0.720 and 0.980, respectively. At t = 0.16 s, the calculated p.u. values for the source and load peak voltages were 1.201 and 1.010, respectively. Hence, voltage was restored to the load for increasing and decreasing source voltage amplitudes.

The responses of the speed and electromagnetic torque shown in Fig. 12 were not same as that from Fig. 7, but show an improved characteristic compared to that from Fig. 10. For t < 0.1 s, the characteristics remained identical with those of the ideal in Fig. 12. Between t = 0.1 s – 0.2 s, the oscillation of the speed was within 1456 ± 82.55 rpm. The torque also oscillated minimally with a peak of 77.7 Nm, at t = 0.12 s. However, there were instances of two subtle pairs of zero-crossings. The persistent oscillation at t > 0.2 s were also damped.

IV. CONCLUSION

From the findings, the conclusions are that load voltage, speed and torque characteristics of the SCIM are useful for qualifying the effects of unbalanced voltage-based vibrations, together with the p.u. calculations. Secondly, the effects of voltage unbalance on vibrations of SCIM were appreciably damped by use of APF filter. Thirdly, the torque overshoot observed while damping was carried out was as a result of the switching mechanism employed in the simulations and lastly, series APF is a useful approach to damping unbalanced voltage-based vibrations

IEEE Office - SEET Complex, Federal University of Technology, Owerri, Nigeria, https://aeuso.org
EISSN: 2305-0543, PISSN: 2411-6173

REFERENCES

[1] D. J. Inman, *Engineering vibration*, Pearson Education, Inc. Upper Saddle River, New Jersey, 4th edition, 707 pp., 2014.

[2] S. S. Rao, *Mechanical vibrations*, Pearson Education, Inc., Harlow, England, 6th edition, 1147 pp., 2018.

[3] W. Finley, M. Loutfi, and B. J. Sauer, "Motor vibration problems - Understanding and identifying", In *Proceedings of IEEE-IAS/PCA Cement Industry Technical Conference*, Orlando, Florida, pp. 1–20, 2013.

[4] P. Donolo, G. Bossio, C. De Angelo, G. García, and M. Donolo, "Voltage unbalance and harmonic distortion effects on induction motor power, torque and vibrations", *Electric Power Systems Research*, Vol. 140, No. 3, pp. 866–873, 2016.

[5] S. Karmakar, S. Chattopadhyay, M. Mitra, and S. Sengupta, "Induction motor and faults", In *Induction Motor Fault Diagnosis*, Springer, Singapore, 1st edition, pp. 7 – 28, 2016.

[6] J. Rangel-Magdaleno, H. Peregrina-Barreto, J. Ramirez-Cortes, R. Morales-Caporal, and I. Cruz-Vega, "Vibration analysis of partially damaged rotor bar in induction motor under different load condition using DWT", *Shock and Vibration*, Vol. 2016, No. 4, pp. 144–155, 2016.

[7] B. Basu, A. Staino, and M. Basu, "Role of flexible alternating current transmission systems devices in mitigating grid fault-induced vibration of wind turbines", *Wind Energy*, Vol. 17, No. 7, pp. 1017–1033, 2013.

[8] Anon., "Most Common Causes of Machine Vibration",M*www.fluke .com/en/learn/ vibration*. Accessed: January 4, ,٢٠١٩ 2013.

[9] S. Payami, R. K. Behera, A. Iqbal, and R. Al-Ammari, "Common-mode voltage and vibration mitigation of a five-phase three-level npc inverter-fed induction motor drive system", *IEEE Journal of Emerging and Selected Topics in Power Electronics*, Vol. 3, No. 2, pp. 349–361, 2015.

[10] D. A. Mistry, B. Dheeraj, R. Gautam, M. S. Meena, and S. Mikkili, "Power quality improvement using pi and fuzzy logic controllers based shunt active filter", *International Journal of Electrical, Computer, Energetic, Electronic and Communication Engineering*, Vol. 8, No. 4, pp. 652–661, 2014.

[11] D. Prasad, and K. B. G. Tilak, "Power quality improvement by using shunt hybrid power filter and thyristor controlled reactor", *International Journal of Scientific Engineering and Technology Research*, Vol. 4, No. 35, pp. 7095–7099, 2015.

[12] U. Werner, "Mathematical multibody model of a soft mounted induction motor regarding forced vibrations due to dynamic rotor eccentricities considering electromagnetic field damping", *Journal of Applied Mathematics and Physics*, Vol. 5, No. 2, pp. 346–364, 2017.

[13] U. Werner, "Vibration control of large induction motors using actuators between motor feet and steel frame foundation", *Mechanical Systems and Signal Processing*, Vol. 112, No. 3, pp. 319–342, 2018.

[14] X. Xu, Q. Han, and F. Chu, "Review of electromagnetic vibration in electrical machines" *Energies*, Vol. 11, No. 7, pp. 1779–1812, 2018.

[15] M. Rosić, B. Jeftenić, and M. Bebić, "Reduction of torque ripple in dtc induction motor drive with discrete voltage vectors", *Serbian Journal of Electrical Engineering*, Vol. 11, No. 1, pp. 159–173, 2014.

[16] C. Dinakaran, "Modelling and simulation of speed control of induction motor by space vector modulation technique using voltage source inverter", *Journal of Electrical Engineering*, Vol. 15, No. 3, pp. 280–287, 2015.

[17] D. Goyal, and B. S. Pabla, "The vibration monitoring methods and signal processing techniques for structural health monitoring: A review", *Archives of Computational Methods in Engineering*, Vol. 23, No. 4, pp. 585–594, 2016.

[18] K. Sebasthirani, and K. Porkumaran, "Performance enhancement of shunt active power filter with fuzzy and hysteresis controllers", *Journal of Theoretical and Applied Information Technology*, Vol. 60, No. 2, pp. 284–291, 2014.

[19] B. P. Ankita, A. B. Rupali, B. G. Rupali, and R. S. Bhushan, "Power quality improvement by series active power filter - A review", *International Research Journal of Engineering and Technology*, Vol. 4, No. 1, pp. 1730–1733, 2017.

[20] P. Korondi, K. Samu, L. Raj, A. Décsei-Paróczi, D. Fodor, J. Vásárhelyi, and J. Vass, "Modelling induction motors", In *Digital Servo Drives*, Budapest University of Technology and Economics, Budapest, 1st edition, pp. 198 – 214, 2014.

[21] A. Bellure, and M. S. Aspalli, "Dynamic d-q model of induction motor using simulink", *International Journal of Engineering Trends and Technology*, Vol. 24, No. 5, pp. 252–257, 2015.

[22] Anon., "Asynchronous Machine", *www.mathworks.com*. Accessed: April 6, 2019, 2019.

[23] A. H. Budhrani, K. J. Bhayani, and A. R. Pathak," Design parameters of shunt active filter for harmonics current mitigation", *Journal of Energy and Management*, Vol. 10, No. 2, pp. 59 – 65, 2018.

IEEE Office - SEET Complex, Federal University of Technology, Owerri, Nigeria, https://aeuso.org
EISSN: 2305-0543, PISSN: 2411-6173